Theoretical Studies on the Intramolecular Hydrogen Bond and Tautomerism of 8-Mercaptoquinoline in the Gaseous Phase and in Solution Using Modern DFT Methods

Andrew E. Shchavlev

Division of Computational and Informational Science,Volga Region Academy of State Service, 23/25 Sobornaya Street, Saratov 410031, Russia

Alexei N. Pankratov* and Alexei V. Shalabay

Department of Chemistry, N. G. Chernyshevskii Saratov State University,83 Astrakhanskaya Street, Saratov 410012, Russia

Received: February 17, 2005; In Final Form: March 15, 2005

A theoretical quantum chemical study of the intramolecular hydrogen bonding interactions in 8-mercaptoquinoline has been carried out. Special attention has been paid to the rotation of S−H bond and intramolecular proton-transfer reactions. Therewith, the B3LYP/6-311++G(d,p), B3LYP/6-31+G(2d,2p), MPW1K/6-311++G(d,p), MPW1K/6-31+G(2d,2p), BH&HLYP/6-311++G(d,p), and G96LYP/6-311++G(d,p) methods have been used. By means of the Onsager and PCM reaction field methods, the effects of solvent on hydrogen-bond energies, conformational equilibria, rotational barriers, and tautomerism in aqueous solution have been studied. These simulations were done at the MPW1K/6-311++G(d,p) and B3LYP/6-311++G(d,p) levels. Natural-bond orbital analysis has been performed to study the intramolecular hydrogen bond (IHB) in the gaseous phase and in aqueous medium. The stability of forms under consideration in solution does not coincide with that in the gaseous phase, underlining a great importance of the electrostatic influence of solvent. Double-proton transfer in the prototropic tautomerization of 8-mercaptoquinoline, one water molecule complex in the gaseous phase and in solution, has been systematically studied. The double-proton transfer occurs concertedly and synchronously. The water-assisted tautomerization is kinetically less, but thermodynamically more favorable, compared to that of the single-proton transfer. As in the case with single-proton transfer, for water-assisted reaction, the tautomerization energies and barrier heights decrease with the increase in dielectric constant, which implies faster and more complete tautomerization of 8-mercaptoquinoline in a polar solvent.

Introduction

For solving modern problems of coordination chemistry, analytical science, development of the theoretical bases of metal ion interaction with organic compounds, of considerable interest is the comparative study of reagents, which are close to each other by structure and differ only by active donor atoms ligating metal. The examples of such reagents are substances containing oxygen, sulfur, and selenium as donor atoms. In this connection, it should be of importance to explore 8-mercaptoquinoline (8-MQ), the sulfur-containing analogue of 8-hydroxyquinoline. The chemistry of intramolecular hydrogen bond (IHB) formation in 8-MQ has been researched widely by various experimental methods,[1−3] but there is the substantial lack of theoretical computational studies in this area.

Barriers of the S−H group rotation between two planar conformations can shed light upon the conditions of IHB formation or cleavage in the 8-MQ molecule.

The 8-MQ explicit capability of forming the zwitterionic tautomer, in contrast to 8-hydroxyquinoline, may be explained by the presence of vacant d-orbitals in the sulfur atom. These orbitals could assist the sulfur atom interaction, by means of $3d_\pi - 2p_\pi$ conjugation, with the quinoline π-system. Because of the electron-acceptor character of 3d-orbitals, the sulfur atom in 8-MQ attracts electrons from the quinoline system, which is confirmed by the dramatic decrease in the basicity of the nitrogen atom[4,5] compared to that of 8-hydroxyquinoline.[4] The clarification of questions related to the formation and structure of the zwitterion of 8-MQ is of great significance for explaining the physicochemical properties of chelates of metals with incompletely occupied d-orbitals.[6] The structural peculiarities of the zwitterionic form and its stabilization in polar solvents may be explained by the formation of molecular complexes of zwitterions with solvent molecules. The polar solvent molecules play a significant role not only in the stabilization of the zwitterionic form. A proton may pass completely from the S−H group to the nitrogen atom under the condition of definite orientation of polar solvent molecules surrounding the 8-MQ molecule. The force field of the intermolecular interaction contributes to the S−H bond polarization via strengthening the IHB and, as a result, reduces the energetic barrier height of complete proton transfer.[7] Because the majority of proton transfers occurs in aqueous solution, it is necessary to consider the role of water molecules in the proton transfer. Water is not solely a solvent, but also a mediator, which gives and accepts protons to promote the large-distance proton transfer. In connection with the aforesaid, it would be useful to consider the double-proton transfer in water-assisted tautomerization of 8-MQ. Such a process has been studied recently by Fang et al.,[8] but only for 8-hydroxyquinoline and for the gaseous phase.

* Author to whom corresponding should be addressed. E-mail: PankratovAN@chem.sgu.ru.

10.1021/jp050838e CCC: $30.25
Published on Web 04/20/2005

The present study focuses on the investigation of such characteristics as the energy of the 8-MQ complexation with water and tautomerization energy as well as the barriers of single and double-proton transfer in the gaseous phase and in solvents (using the self-consistent reaction field approach). We believe that these results obtained for such a model system as the 8-MQ−H_2O complex may be useful for further systematic studies of various species reactivity in processes involving double-proton transfers in hydrogen-bonded complexes.

The paper is organized as follows. The Computational Methods section outlines the computational details. Sections 1.1 and 1.2 present the geometry, IR spectra, and relative stability of rotamers and tautomers of 8-mercaptoquinoline. Section 1.3 demonstrates the reaction barriers, and section 1.4 shows the Mulliken charge distribution and dipole moments. In Section 1.5, the natural bond orbital (NBO) analyses are considered. Section 2.1 presents the water-assisted tautomerization in the gaseous phase and in various media. Section 2.2 examines the NBO analysis of the 8-MQ−H_2O complex. Finally, the Conclusions section outlines the summary remarks.

Computational Methods

All calculations of electronic structure in this paper were carried out using the Gaussian 98W package.[9] Four different self-consistent field-density functionals were used for the calculations: the hybrid B3LYP functional, which combines the three-parameter exchange functional of Becke[10] with the LYP correlation one;[11] the hybrid model called the modified Perdew-Wang one-parameter model for kinetics (MPW1K);[12] the hybrid Half-and-Half (BH&HLYP) functional;[13] one-parameter hybrid functional with Gill 96 exchange, and LYP correlation functional (G96LYP).[14] The computations were performed using tight convergence criteria.[15] The 6-31G(d,p),[16] 6-31+G(2d,2p),[17,18] and 6-311++G(d,p)[19,20] basis sets were used. The initial geometries were generated by HyperChem (HyperChem, Hypercube, Inc., Gainesville, FL 32601, U.S.A.) and optimized in three steps. On the first step, the geometry was optimized using the restricted Hartee−Fock method with the STO-3G basis set. No geometrical constraints were imposed on the molecules. The second optimization step was performed using the B3LYP/6-31G(d,p) level. The final optimizations were performed at B3LYP/6-311++G(d,p), B3LYP/6-31+G-(2d,2p), MPW1K/6-311++G(d,p), MPW1K/6-31+G(2d,2p), and BH&HLYP/6-311++G(d,p) levels. Harmonic vibrational frequencies were computed to evaluate the zero-point energy (ZPE) corrections, which we have included in all the relative energies. The transition-state calculations used the synchronous transit-guided quasi-Newton (STQN) method.[21] For all the transition states, the existence of imaginary frequencies[22] were stated, and then a further characterization of the transition states was achieved by calculation of the intrinsic reaction coordinate (IRC).[23] leading to the corresponding energy minima. NBO analysis has been performed by the NBO 3.1 program.[24]

Specific interaction between the solute (8-MQ) and the solvent (water) was considered at the B3LYP/6-311++G(d,p), MPW1K/6-31+G(2d,2p), BH&HLYP/6-311++G(d,p), and G96LYP/6-311++G(d,p) theory levels. The formation energies for the water-containing complexes were calculated as the differences in energies between the complex 8-MQ−H_2O and two separate molecules, 8-MQ and H_2O. For such energy estimations, the basis set superposition error (BSSE) holds much significance. The BSSE was corrected by the Boys and Bernardi counterpoise correction scheme:[25]

$$\mathrm{BSSE} = [E(\mathrm{A})_{\mathrm{AB}} + E(\mathrm{B})_{\mathrm{AB}}] - [E(\mathrm{A})_{\mathrm{A}} + E(\mathrm{B})_{\mathrm{B}}]$$

where $E(A)_{AB}$ and $E(B)_{AB}$ are the energies of the separate molecules A and B calculated with the full basis set of the AB complex under the zero charges of imaginary atoms, the spatial positions of which coincide with those in the AB complex, and the $E(A)_A$ and $E(B)_B$ are the energies of the separate molecules A and B with their own basis sets.

The SCRF theory[26] was used to optimize the structures and to calculate the energies for 8-MQ and 8-MQ−H_2O complex at different values of dielectric constants. Frequencies were calculated for both the ground and transition states. In the Onsager model,[27] the radius of the solute molecular system was calculated from the molecular volume for the structure optimized in the gaseous phase. The polarizable continuum model (PCM) was also used.[28] In this approach, the solute, treated quantum chemically, is placed in a cavity surrounded by the solvent. The latter is considered as a continuum characterized by such its bulk property as a dielectric constant. The standard PCM calculations of the solvation energies with 60 initial tesserae per atomic sphere were performed, and the UAHF[29] model was also applied using the Pauling set of atomic radii.

Results and Discussion

1. Rotation Barriers and Tautomerization. *1.1. Conventional Analysis of the Geometry Data and IR Spectrum.* The computed geometries of various forms of 8-MQ (Figure 1) are presented in Table 1. The parameters optimized by the B3LYP/6-311++G(d,p) and MPW1K/6-311++G(d,p) methods are in line with each other. The molecular systems I−III belong to the C_s symmetry point group, and the transition states TS1 and TS2 to the C_1 group. The molecules I−III possess planar structure in the gaseous phase. The carbon atoms, along with the S−H and N−H bonds, lie in one plane. Thus, the conjugate system includes all the carbon atoms and heteroatoms. In molecule I, the S−H bond distance is 1.351 Å (B3LYP) and 1.339 Å (MPW1K). In passing to the II conformer, this bond lengthens a little, and the increase in S11−N1 internuclear distance is also observed. The most important internuclear distances responsible for proton transfer are N1−H12 and S11−N1. On the proton-transfer II → III, the distance between sulfur and hydrogen (S11−H12) enlarges, and between nitrogen and hydrogen (N1−H12) reduces. The results obtained show that the distance between sulfur and nitrogen (S11−N1) becomes longer in going from I to II and shorter on the II → III transfer. The distances between the nitrogen atom and labile hydrogen atom in II, as well as between the sulfur atom and the same hydrogen atom in III, are close to 2 Å. Therefore, according to the computations at all the theory levels applied, the IHB exists in the systems II and III. In the series I → II → III, the decrease in C7−S11 distance takes place. The angle ∠(C7−C6−N1) diminishes greatly when passing from II to III. In the system III, the C−S bond gains a double character to some extent compared to that of I and II. As can be seen from Table 1, the solvent reaction field exerts some influence on the geometry of molecules under investigation. In the aqueous solution, the geometries of I−III appear to be slightly nonplanar. In comparison with the gaseous-phase calculations, one could observe some deviations of dihedral angles listed in Table 1 from the plane of quinoline system. The calculated N1−H12, S11−H12, S11−C7, and S11−N1 distances in the I−III species have been found to alter slightly in going from the gaseous phase to solution. In particular, for the tautomer III, these bonds (except for N1−H12, which shortens) lengthen by about 0.05−0.1 Å.

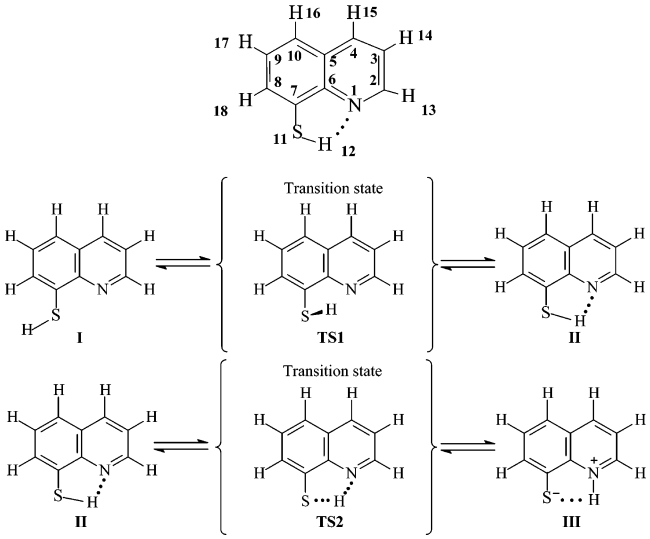

Figure 1. Structures of rotamers and tautomers of 8-mercaptoquinoline.

In aqueous medium against the gaseous phase, in the molecule I, the hydrogen bond N1···H12 becomes longer by 0.06 Å, and in the III molecule, the hydrogen bond S11···H12 becomes shorter by about 0.14 Å. The most severe change in the reaction field is observed for the ∠(C6−N1−H12) angle. This angle decreases by ∼ 4° in moving from the gaseous phase to solution.

Some bands of the IR spectrum of 8-MQ (structures II and III) are shown in Table 2. The numerical values of experimental[30,31] vibrational frequencies have been compared with the theoretical ones. One could see that the ν(S−H) vibration in II is pure, i.e., it is not mixed with any other mode. The latter is confirmed by the experimental data.[7] As is known,[7] the ν(S−H) band, measured in dilute solution and in liquid film, does not dependent upon concentration. This fact allows one to conclude that, for the form II of 8-MQ, the band of moderate intensity in the area of 2535−2500 cm^{-1} should be assigned to the ν(S−H) vibration perturbed by the S−H···N IHB.[32] In the case of structure III, the ν(N−H) band (Table 2) also represents a pure vibrational mode and is perturbed by the N−H···S IHB, which is in agreement with the experimental data.[7] Among the approaches used, the most applicable one for reproducing the IR spectrum of 8-MQ seems to be the B3LYP/6-311++G(d,p) theory level.

Direct correct computation of vibrational frequencies is a very complicated problem requiring the ab initio or DFT approach. Therewith, the Hartree−Fock method dramatically (by 200−500 cm^{-1}) overestimates the high frequencies (≥1600 cm^{-1}), considerably underestimates low ones (≤300 cm^{-1}), and systematically (by 100−200 cm^{-1}) overestimates the rest because of nonallowance for electron correlation.[33,34] The latter, even being considered within the framework of MP2 theory, does not contribute to the better situation. The DFT (B3LYP) method is much more successful in simulating the aforesaid values: high frequencies (≥1600 cm^{-1}) are overestimated 100−150 cm^{-1}, low frequencies (≤300 cm^{-1}) are underestimated to a lesser extent, and moderate ones (300−1600 cm^{-1}) are overestimated 20−50 cm^{-1}. However, the hybrid character of DFT (presence of a semiempirical component) in a number of cases leads to greater errors for low frequencies (≤ 500 cm^{-1}) and to the nonpredictable asymptotic behavior of adiabatic potential at long internuclear distances.[35] For poor-symmetry molecules, the frequency computation is severely complicated by the anharmonic disturbances as those of the Fermi resonance type by the presence of composed frequencies and a decreased number of experimental criteria of assignment. Besides, on the difference between vibrational level energies comparable to the quantum chemical method error (20−50 cm^{-1} with respect to DFT), accidental coincidence between the computed and experimental frequencies is possible.

For all the frequencies presented in the Table 2, the most adequate evaluations have happened to be those performed by means of the B3LYP method. Under this condition, the errors appear to be within the limits pointed out in the works.[34,35] As for the frequencies of N−H and C−S valent vibrations, the latter item is valid also for the MPW1K and BH&HLYP methods. It is important to note that the B3LYP computations reproduce well the experimental ν(N−H) and ν(C−S) values without scaling.

1.2. Relative Stability of Rotamers and Tautomers of 8-Mercaptoquinoline. The results of the gaseous-phase calculations (Table 3) of three possible species I−III using different DFT methods and basis sets indicate that the most stable structure is the II one. The least stable tautomer is III, 8−12 kcal/mol in relation to II. These results show that only the form II should be present in the gaseous phase. The hydrogen-bond energy is estimated by comparing the energies between the conformer with the hydrogen bond and the rotamer, in which the SH group is rotated by 180° to prevent hydrogen bonding. The most successful result with respect to the IHB energy, about 2.3 kcal/mol (difference of sums of electronic and thermal enthalpies, including ZPE corrections), was computed using the MPW1K/6-311++G(d,p) level. The experimentally observed value of the IHB enthalpy is 2.8 kcal/mol.[36,37] Despite the larger number of the basis functions in the 6-31+G(2d,2p) basis set compared to that of the 6-311++G(d,p) one, computations with the 6-31+G(2d,2p) basis set underestimate the IHB energy. To study the relative stability of the different tautomers in aqueous solution, the solvation effect has been considered via the SCRF method, which provides a simple description of the complex process of solvation. The first variant of the above method used is based on Onsager's reaction field theory, and another one corresponds to the polarizable continuum model (PCM). The solvent effect on the IHB and tautomerism is given in Table 4, where the energies of the solvated 8-MQ species in water (dielectric constant $\epsilon = 78.39$) are presented. It can be inferred from this table that the stability order of the forms in aqueous solution does not strongly depend on the method used to simulate the solvent. However, when using the Onsager model, the stabilizing effect of the solvent upon IHB takes the value of −0.256 kcal/mol, but the increase in IHB energy in the aqueous solution is unlikely. In the case of PCM, the above value is 1.456 kcal/mol. The polar solvent should stabilize preferably the structure III with a higher dipole moment (Table 7), and the SCRF calculations predict that the III form is favored over II in aqueous solution.

The Onsager model failure for the IHB energy variation trend when changing a solvent, could be due to the assumption of a spherical cavity. Because the molecule is planar, the spherical cavity is not adequate; moreover, the Onsager approach requires that the electric dipole is located at the cavity center, which is not true in most cases.

Nevertheless, the results obtained are indicative of the similar performance of the SCRF methods, i.e., the Onsager and PCM models, when treating the II → III tautomerization. The tautomer III predominates in aqueous solution. Obviously, there is the extremely valuable solvent contribution to the tautomer III stabilization. Consequently, the tautomerization reaction proceeds in a greater degree in polar media, which corresponds to

TABLE 1: Selected Optimized Geometries for Rotamers and Tautomers of 8-Mercaptoquinoline at Different Theory Levels[a]

	I			II			III		
	A	B	C	A	B	C	A	B	C
				Bond Lengths (Å)					
N1−H12				2.187	2.156	2.193	1.042	1.044	1.037
S11−H12	1.351	1.339	1.353	1.353	1.342	1.355	2.245	2.173	2.382
S11−C7	1.778	1.756	1.781	1.773	1.751	1.777	1.721	1.705	1.741
S11−N1	2.889	2.582	2.912	3.022	2.985	3.018	2.919	2.867	2.971
				Bond Angles (deg)					
∠(C7−S11−H12)	94.823	94.928	95.550	93.720	93.900	94.319			
∠(C6−N1−H12)				91.153	91.417	91.448	110.206	109.435	114.054
∠(C6−C7−S11)	116.423	116.926	116.892	120.833	120.666	120.542	119.527	118.978	119.889
∠(C8−C7−S11)	124.220	124.364	123.368	119.913	120.108	119.800	126.669	127.273	125.300
∠(C6−N1−C2)	118.398	118.392	118.339	118.894	118.889	118.787	124.817	124.627	124.537
∠(C7−C6−N1)	118.151	117.881	118.626	119.091	118.887	119.207	116.989	116.365	118.608
∠(N1−H12−S11)				115.203	115.131	114.481	120.465	121.966	114.909
				Dihedral Angles (deg)					
∠(C5−C6−C7−S11)	180	180	179.556	−180	−180	−179.675	180	180	179.586
∠(C6−C7−S11−H12)	180	180	176.631	0	0	0.583			
∠(C3−C2−N1−H12)							180	180	179.006

[a] A: B3LYP/6-311++G(d,p); B: MPW1K/6-311++G(d,p); C: B3LYP/6-311++G(d,p) in aqueous solution within the SCRF PCM method.

TABLE 2: Theoretical (Unscaled) and Experimental (in Carbon Tetrachloride) Vibrational Frequencies (cm^{-1}) of 8-Meraptoquinoline and Its Zwitterionic Form

level	ν(S−H)	ν(N−H)[a]	ν(C−H)	ν(C−S)
B3LYP/6-311++G(d,p)	2628	3019	3143, 3164, 3166, 3175	671
MPW1K/6-311++G(d,p)	2738	3072	3232, 3253, 3263, 3277	690
BH&HLYP/6-311++G(d,p)	2764	3210	3243, 3260, 3263, 3270	695
exp[b]	2520	3000	3025−3060	659

[a] The ν(N−H) band, which is present in the zwitterionic structure III.[7] Registered for methyl and phenyl derivatives of 8-mercaptoquinoline in the crystal state. [b] The experimental IR data in carbon tetrachloride are attributed to the structure II.[30−32]

the experimental data.[1] According to Albert et al.,[1] about 96% of zwiterionic form III exists in an aqueous solution of 8-MQ.

1.3. Reaction Barriers. Table 5 contains the calculated gaseous-phase energy differences (rotational barriers) between the transition structure (TS1) and the stable I and II conformers. The values of the I → II rotation barrier calculated using the B3LYP, MPW1K, and BH&HLYP methods with different basis sets are within the range of 3.384−4.132 kcal/mol. As a reference method for the most precise computations of the transition states, MPW1K was chosen, which simulates quite adequately both the geometry of saddle-point structure and the barrier heights.[38] The conformer II would occur promptly from I. The reverse rotation (II → I) barrier has a value of 5.205−6.203 kcal/mol. In the transition state of the I → II and II → I processes, the dihedral angle ∠(C6−C7−S11−H12) is ∼104°; thus, the SH group is turned drastically to the plane of the quinoline system.

The proton-transfer reaction II → III has been studied in this paper. As mentioned above, the proton transfer may occur in 8-MQ because of a short distance (about 2 Å) between N1 and H12. The transition state (referred to as TS2) for prototropic tautomerization was computed, and the existence of a first-order saddle point was proved. This transition state, similarly to the II and III tautomers, has a planar structure. In the gaseous phase, the N1−H12 distance is 1.258 Å, whereas the S11−H12 distance is 1.684 Å (MPW1K/6-311++G(d,p)). Thus, one should believe that the S−H bond is broken, and the N−H bond appears in the transition state. This reaction is severely endothermic, and the transition state geometry (in accordance with the Hammond postulate) is close to that of the product. The MPW1K/6-311++G(d,p) barrier heights for the II → III and III → II reactions are 10.585 and 0.101 kcal/mol, respectively. Evidently, because of a very low barrier, the reverse proton transfer would proceed very readily. The barrier heights for both of the processes II → III and III → II are somewhat dependent on the theory level. Our calculations predict that the proton transfer from II to III is difficult to observe experimentally in the gaseous phase. We have theoretically considered also the above reaction in the aqueous solution. In TS2, N1−H12 lengthens by 0.054 Å (against the gaseous phase), whereas the S11−H12 distance shortens by 0.055 Å. The barrier height for II → III reaction decreases by 2.741 kcal/mol, and the barrier height for the reverse process increases by 4.292 kcal/mol. The process II → III is kinetically and thermodynamically more favored in a polar solvent, and the III tautomer is more stable compared with that of II in aqueous solution, which agrees with the experimental results.[7]

1.4. Mulliken Charge Distribution and Dipole Moments. Starting from the Mulliken population analysis,[39] we have explored the charge distribution in the species I−III for both the gaseous phase and a polar medium. Total atomic charges in the possible rotamers and tautomers of 8-MQ are summarized in Table 6. Our consideration involves the charges on labile hydrogen, as well as on sulfur and nitrogen atoms. According to the gaseous-phase computations, in the course of rotation (I → II) and proton transfer (II → III), a positive charge on the hydrogen atom H12 of S−H group increases slightly, while on the adjacent nitrogen, the positive charge diminishes as a result of rotation (I → II) and grows on the proton transfer (II → III). As for the sulfur atom, it gains a considerable additional negative charge during the reactions I → II and II → III. The charge distribution in the structures under study often changes essentially when acted upon by a solvent reaction field. We examined the charge distribution using the Onsager and PCM models. Water served as a polar medium. Within the framework of the PCM model, the charge distribution in the I−III systems was found to be influenced by the dielectric medium. In the case of the Onsager model, such influence is less profound. It is remarkable that the electron distribution on the S11, N1, and H12 atoms (PCM model) is perturbed by the reaction field. Hence, the solvent should affect the internuclear distances.

TABLE 3: Total[a] (*E*) (a.u.) and Relative to II (ΔE, ΔH) (kcal/mol) Energies for Rotamers and Tautomers of 8-Mercaptoquinoline in the Gaseous Phase Including Zero-point Energy (ZPE) Correction

	I			II		III		
level	*E*	ΔE	ΔH[b]	*E*	ΔE	*E*	ΔE	ΔH
B3LYP/6-31G(d,p)	−799.948500	2.071	2.112	−799.998151	0	−799.984112	8.810	8.599
B3LYP/6-311++G(d,p)	−800.112109	1.857	1.994	−800.115069	0	−800.100064	9.416	9.198
B3LYP/6-31+G(2d,2p)	−800.021105	1.795	1.852	−800.023966	0	−800.009436	9.118	8.899
MPW1K/6-311++G(d,p)	−799.976522	2.218	2.311	−799.980057	0	−799.963350	10.484	10.250
MPW1K/6-31+G(2d,2p)	−799.899567	2.063	2.099	−799.902854	0	−799.886699	10.137	9.894
BH&HLYP/6-311++G(d,p)	−799.833972	1.821	1.877	−799.836874	0	−799.817381	12.232	11.978

[a] Sum of electronic and zero-point energies. [b] Differences of sums of electronic and thermal enthalpies.

TABLE 4: Energies of Hydrated Forms of 8-Mercaptoquinoline Using Different SCRF Methods

form	Onsager model; MPW1K/6-311++G(d,p)	PCM; B3LYP/6-311++G(d,p)
	Total Energies	
I	−799.977738[a](−800.117729)[b]	−800.257638[c]
II	−799.981682 (−800.122686)	−800.258277
III	−799.976183 (−800.140171)	−800.259117
	ΔE[d]	
I	2.475 (3.111)	0.401
II		
III	3.451 (−10.972)	−0.527
	ΔH[e]	
I	2.587	
II		
III	3.210	
	Processes; Transition States; Barriers[f]	
TS1: I → II	3.029	
TS1: II → I	2.113	
TS2: II → III	7.844	
TS2: III → II	4.393	

[a] Sums of electronic and zero-point energies in Hartree/particle. [b] Total energies of solute (SCRF *E*-field) in Hartree/particle. [c] Total energies of the polarized solute (PCM) in Hartree/particle. [d] Relative to II energies in kcal/mol. [e] Differences of sums of electronic and thermal enthalpies in kcal/mol. [f] Relative to II energies in kcal/mol.

Indeed, in the molecule II, the N1···H12 distance (PCM:B3LYP/6-311++G(d,p)) lengthens slightly in aqueous medium compared to that of the gaseous phase. The energy released because of the dipole−dipole interaction between polar solvent and solute molecules is sufficient to lose considerably the intramolecular forces in solution. Thus, the hydrogen bond is weaker to a somewhat greater extent in polar solvent.

A comparison within the data of Table 7 shows that the dipole moment values are scantily dependent on the computation level. For all the species, the differences in dipole moments in solution are more pronounced than those in the gaseous phase. It could be mentioned also that the calculated dipole moment of the molecular system III is much higher than that for II and I. Hence, the reaction field exerts a greater effect on the III structure and makes III more preferable in aqueous solution[7] as is discussed below.

On the basis of the comparison of dipole moments at different concentrations of zwitterionic forms of 8-MQ and its derivatives in solution, it has been proposed[7,40,41] that the capability of these compounds of forming zwitterions is governed to a great extent by the value of the dipole moment vector of the II form, and the direction of the dipole moment vector determines the functional groups of 8-MQ, with which the solvent molecules interact. We have computed the direction of the dipole moment vector (Figure 2). The force field of the solvent molecules interacting with the form II promotes the polarization of the S−H bond and proton transfer to the nitrogen atom of the quinoline system.

1.5. NBO Analysis. The natural bond orbital (NBO) analysis of the IHB for II and III structures was carried out in the gaseous phase and in aqueous solution. The contributions involving the lone electron pairs of nitrogen and sulfur were taken into account. The results are presented in Table 8. We considered the interactions with the energy exceeding 5 kcal/mol. The stabilization energies were estimated by analyzing the interactions between the "filled" Lewis-type NBOs and the "empty" non-Lewis NBOs. Our findings are indicative of the occurrence of interactions resulting in a small electron-density transfer from the localized NBOs of the idealized Lewis structure into the empty non-Lewis orbitals. The set of 42 substantially occupied NBOs consists of 97% of the electron density for II and III structures in both media. The results show that the delocalization interactions are especially considerable for the π−system and for the lone pairs (*n*) of the nitrogen and sulfur atoms.

In the processes of the electron transfer in the structure II, the following interactions are observed: the electron transfer from the lone pair of N1 to the antibonding orbitals C5−C6 and C2−C3 as well as from the antibonding orbital C5−C6 to the C7−C8 and C9−C10 antibonding orbitals. Besides, a contribution representing the electron transfer from the lone pair of S11 to the antibonding orbital C7−C8 appears. Thus, the charge transfer from the lone pairs of the electron donors (N and S) and antibonding orbitals of the molecule's central part is directed mainly to the antibonding orbitals of the remote part of the compound. The latter agrees with the results discussed in the review.[42] It is interesting that the antibonding C5−C6 → C7−C8 interaction becomes appreciable only in aqueous solution.

The most essential delocalization in the structure III between the lone pair of S11 and the antibonding orbitals C6−C7 and N1−H12 should be regarded as the IHB manifestation leading to the formation of a five-membered quasiring.

The effect of the IHB has been studied by comparing two conformers I and II. We assume that the differences in the charges obtained by the NBO analysis, as well as in Wiberg bond orders, reflect the effect of IHB on the electron density distribution in the molecule. The changes in the natural charges and in the bond orders of II with respect to I from B3LYP/6-311++G(d,p) calculations in the gaseous phase and in aqueous solution are depicted in Figure 3. The charge distribution of II shows that the weak (compared to that of I) character change of the bonds involved in the hydrogen-bonded five-membered quasicycle takes place. The electron density on sulfur and nitrogen atoms increases and on labile hydrogen diminishes, the smaller change being in aqueous solution. In the latter, the greatest increase in the electron density is observed on C7, and some diminution on C5 and C6. The involvement of C5, C6, and C7 atoms in the electron density changes in solution, in contrast to that of the gaseous phase, is in agreement with significant $BD^*(C5-C6) \rightarrow BD^*(C7-C8)$ donor−acceptor

TABLE 5: Rotation and Intramolecular Proton-transfer Barriers (kcal/mol) Including Zero-point Corrections

process and transition state	B3LYP/6-31G(d,p)	B3LYP/6-311++G(d,p)	B3LYP/6-31+G(2d,2p)
TS1: I → II	4.132	4.083	4.108
TS1: II → I	6.203	5.941	5.904
TS2: II → III	9.405	10.257	9.802
TS2: III → II	0.596	0.841	0.685
process and transition state	MPW1K/6-311++G(d,p)	MPW1K/6-31+G(2d,2p)	BH&HLYP/6-311++G(d,p)
TS1: I → II	3.683	3.742	3.384
TS1: II → I	5.901	5.804	5.205
TS2: II → III	10.585	10.192	14.072
TS2: III → II	0.101	0.055	1.839

TABLE 6: Mulliken Charges on Sulfur, Nitrogen and Labile Hydrogen

	I			II			III		
method	N1	H12	S11	N1	H12	S11	N1	H12	S11
B3LYP/6-31G(d,p)	−0.505	0.037	0.062	−0.545	0.106	−0.011	−0.523	0.275	−0.366
B3LYP/6-311++G(d,p)	0.203	0.102	−0.464	0.107	0.162	−0.612	0.426	0.237	−1.146
PCM: B3LYP/6-311++G(d,p)	0.104	0.152	−0.525	0.045	0.181	−0.641	0.299	0.323	−1.232
B3LYP/6-31+G(2d,2p)	0.038	0.077	−0.461	−0.001	0.137	−0.519	0.374	0.191	−0.910
MPW1K/6-311++G(d,p)	0.288	0.138	−0.586	0.184	0.195	−0.777	0.537	0.278	−1.368
Onsager: MPW1K/6-311++G(d,p)	0.285	0.134	−0.614	0.180	0.196	−0.816	0.461	0.300	−1.518
MPW1K/6-31+G(2d,2p)	−0.030	0.075	−0.442	−0.062	0.134	−0.479	0.297	0.206	−0.916
BH&HLYP/6-311++G(d,p)	0.182	0.100	−0.430	0.078	0.157	−0.593	0.359	0.251	−1.168

TABLE 7: Dipole Moments (D) for Different Forms of 8-Mercaptoquinoline

method	I	II	III	exp[a]
B3LYP/6-31G(d,p)	2.759	3.081	7.540	
B3LYP/6-311++G(d,p)	2.729	3.017	7.561	
B3LYP/6-31+G(2d,2p)	2.681	2.954	7.492	
MPW1K/6-311++G(d,p)	2.822	3.186	8.001	2.89
MPW1K/6-31+G(2d,2p)	2.772	3.114	8.006	
BH&HLYP/6-311++G(d,p)	2.896	3.195	8.415	
Onsager: MPW1K/6-311++G(d,p)	3.665	4.299	12.515	
PCM: B3LYP/6-311++G(d,p)	4.070	4.509	11.329	

[a] Measured by the second Debye method in benzene solution at 25°.[40]

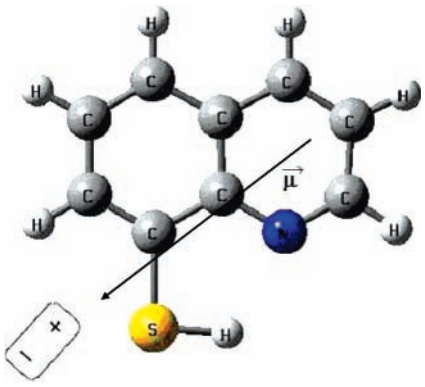

Figure 2. Dipole derivative unit vector $\vec{\mu}$ direction for the structure II (B3LYP/6-311++G(d,p)).

interactions occurring only in the aqueous medium. The latter interaction may be a result of a strong augmentation of the attractive electrostatic terms and solvent polarization. The charges on the other ring carbons do not alter under the above intramolecular interaction. Among the parameters of II, the S11−H12 bond order shows a significant decrease, and the C7−S11 bond order increases appreciably as a result of the IHB formation. These tendencies occur in both media.

We have also considered the changes of charge distributions and Wiberg bond orders in III with respect to II from NBO analysis at the B3LYP/6-311++G(d,p) level both in the gaseous phase and in aqueous medium (Figure 4). As for both said media, we may verify that the charge distribution of III shows (compared to that of II) a strong polarization of the bonds involved in the hydrogen-bonded five-membered ring.

TABLE 8: Second-order Perturbation Energies *E*(2) (kcal/mol)

NBO		energy	
donor	acceptor	II	III
LPN1	BD*(C5−C6)	9.56	
LPN1	BD*(C2−C3)	9.37	
BD*(C5−C6)	BD*(C7−C8)	223.45[a]	
BD*(C5−C6)	BD*(C9−C10)	218.68	
LPS11	BD*(C7−C8)	19.08	7.87
LPS11	BD*(C6−C7)		6.47
LPS11	BD*(N1−H12)		15.01

[a] Only in solution (SCRF PCM).

We note that, in the gaseous medium, there is a considerable electron density decrease on the hydrogen atom H12 and a large increase on the sulfur one. Significant changes in electron density is also observed on C4, C6, C7, and C10 atoms. The charges on the other ring carbons are not influenced greatly by the above proton-transfer interaction. The S11−C7 bond order shows a marked augmentation and gains a double character to some extent as a result of the tautomerization. The C7−C8 and N1−C2 bond orders display a considerable diminution.

In the aqueous medium, one can see the increase of charge separation between the nitrogen and sulfur atoms compared to that of the gaseous phase. Namely, the enlargement of the negative charge on S11 and positive charge on N1 takes place. This effect corresponds to the well-known trend of the influence of polar solvents upon charge distribution in molecules. The partially double character of the S11−C7 bond decreases on passing to the aqueous solution. Also, the charges on C5, C7, and C12 atoms, as well as on the C7−C8, C8−C9, and C9−C10 bond orders undergo rather considerable alterations on going from gas to polar solvent. Thus, the aqueous medium leads, besides the S11 and N1 atomic charge alterations, to the more significant changes of electron-density distribution just in the aromatic, not heteroaromatic, ring in comparison with that of isolated molecular systems.

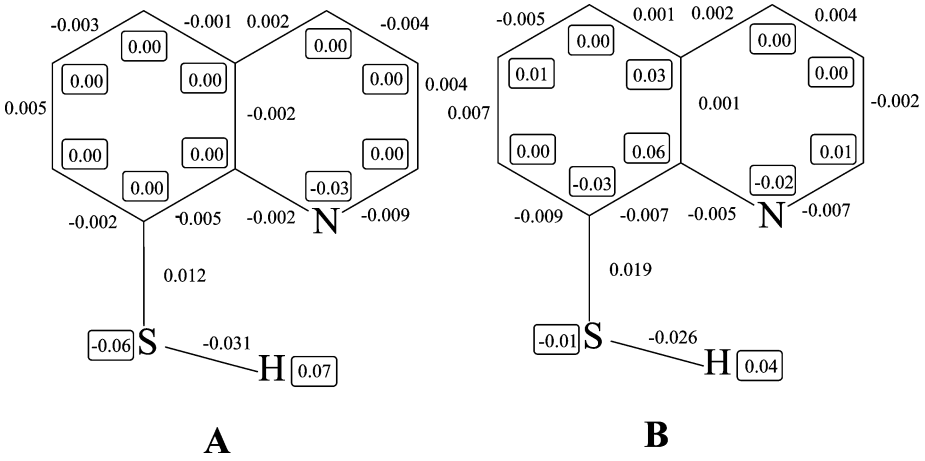

Figure 3. Changes in natural charges (circled, in atomic units) and Wiberg bond orders in II with respect to I from NBO analysis at the B3LYP/6-311++G(d,p) level in the gaseous phase (A) and in aqueous solution (B) using the PCM method.

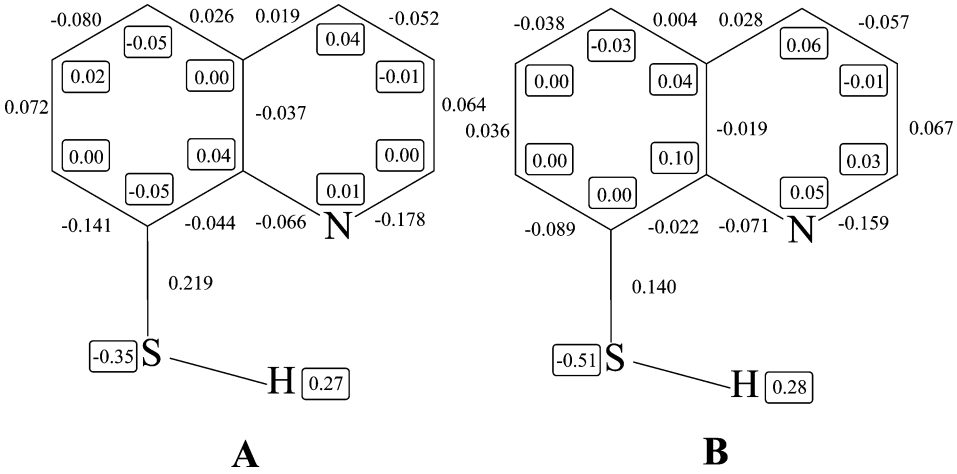

Figure 4. Changes in natural charges (circled, in atomic units) and Wiberg bond orders in III with respect to II from NBO analysis at the B3LYP/6-311++G(d,p) level in the gaseous phase (A) and in aqueous solution (B) using the PCM method.

2. Water-assisted Tautomerization. *2.1. Structures and Energies of Tautomers.* As an alternative way for proton transfer in 8-MQ, let us consider the double-proton transfer in hydrogen-bonded complex of 8-MQ with one water molecule (8-MQ−H_2O) in the gaseous phase and in solution. The equilibrium nonplanar geometry of 8-MQ−H_2O in the ground state was obtained at different DFT levels for the forms IV and V. Our computations of vibrational frequencies have confirmed that the above geometry corresponds to the minima of potential energy surface. The gaseous-phase spatial parameters for the systems IV and V and the transition state TS3 are shown in Table 9. In general, the bond lengths and valence angles calculated by the different methods are close to each other. The computations at any theory level used predict that all the structures should be assigned to the C_1 symmetry point group. As can be seen from Table 9, the hydrogen-bonded structures IV and V of 8-MQ−H_2O differ substantially from those of 8-MQ. There are two intermolecular H-bonds, S11−H12···O19 and O19−H20···N1 in the molecule IV, and O19−H12···S11 and O19···H20−N1 in V. In these systems IV and V, the H_2O molecule serves as a bridge between the ring nitrogen atom (or NH group) and the SH group (or S^-). This is clearly indicative of the cooperative character of the two hydrogen bonds in IV and V. The above effect is commonly associated with donor−acceptor interactions, in which a molecule can participate concertedly as a donor and an acceptor.[43] On the hydrogen bond formation, the S11−H12 bond in IV and N1−H20 in V shorten. The S11−O19 and O19−N1 distances are 3.686 Å and 2.888 Å (IV), and 3.212 Å and 2.887 Å (V), respectively (MPW1K/6-311++G(d,p)), which are longer than the S11−N1 distance in 8-MQ equal to 2.985 Å (II) and 2.867 Å (III). The H12−O19 and N1−H20 distances in IV are 2.512 Å and 1.930 Å, respectively, and the N1−H12 distance in II is 2.156 Å. Because the S11−O19 and H12−O19 distances in IV are significantly greater than S11−N1 and N1−H12 in II, the proton transfer in the complex could be predicted to be hampered in comparison with the individual 8-MQ molecule. However, this question will be discussed below on the basis of the calculated barrier heights. After the 8-MQ−H_2O complex formation, the proton-transfer reaction may involve H_2O as a bridge. It is easily seen from the complex 8-MQ−H_2O structure in Figures 5 and 6 that the H12 proton attached initially to S11 then transfers to O19, and simultaneously, the second proton H20 moves from O19 to N1. To clear up a question whether any high-energy intermediate exists along the reaction path, we have computed the intrinsic reaction coordinate for double-proton transfer at the B3LYP/6-311++G(d,p) level starting from the transition state TS3. The results are shown in Figure 7. There is no intermediate along the intrinsic reaction coordinate, and the reaction proceeds smoothly from reactant to product. It is safe to say in this connection that two protons in the gaseous phase transfer concertedly and synchronously. In the transition state TS3, both protons of the water molecule are disposed closely to the oxygen atom.

TABLE 9: Selected Optimized Geometries for Tautomers and Transition State of Tautomerization of the 8-MQ Complex with One Water Molecule in the Gaseous Phase at Different Theory Levels[a]

	IV		V		TS3	
	A	B	A	B	A	B
			Bond Lengths (Å)			
N1−H20	1.953	1.930	1.032	1.025	1.303	1.311
N1−C6	1.363	1.350	1.363	1.350	1.370	1.358
C6−C7	1.433	1.422	1.441	1.427	1.443	1.431
S11−C7	1.776	1.755	1.728	1.711	1.761	1.742
S11−H12	1.347	1.337	2.319	2.308	1.651	1.658
S11−N1	3.107	3.056	3.074	3.012	3.227	3.184
O19−H12	2.485	2.512	0.983	0.970	1.205	1.164
O19−H20	0.975	0.963	1.900	1.0.901	1.179	1.146
			Bond Angles (deg)			
∠(C7−S11−H12)	97.519	97.285	114.389	115.387	102.258	102.764
∠(C6−N1−H20)	138.720	138.760	117.408	116.636	123.401	123.845
∠(C6−C7−S11)	123.302	122.709	123.353	122.570	126.986	126.716
∠(S11−H12−O19)	150.806	144.787	150.627	150.027	165.798	165.475
∠(C6−N1−C2)	119.125	119.161	124.991	124.879	122.003	121.865
∠(C7−C6−N1)	120.128	119.776	119.611	118.886	121.458	121.187
∠(N1−H20−O19)	169.441	168.140	158.733	155.814	172.965	172.887
∠(H12−O19−H20)	50.732	49.076	73.541	71.839	86.219	86.380
∠(H20−O19−H21)	105.495	105.587	126.275	128.835	108.122	111.514
			Dihedral Angles (deg)			
∠(C5−C6−C7−S11)	−179.439	−179.758	−179.535	−179.541	−176.886	−177.637
∠(C6−C7−S11−H12)	13.496	17.317	7.077	7.321	−6.414	−3.695
∠(C3−C2−N1−H20)	170.979	170.125	179.682	179.411	175.945	177.083
∠(S11−H12−O19−H20)	86.568	84.175	11.417	13.610	4.302	7.614
∠(N1−H20−O19−H12)	102.955	109.033	153.965	155.120	15.264	15.982

[a] A: B3LYP/6-311++G(d,p); B: MPW1K/6-311++G(d,p).

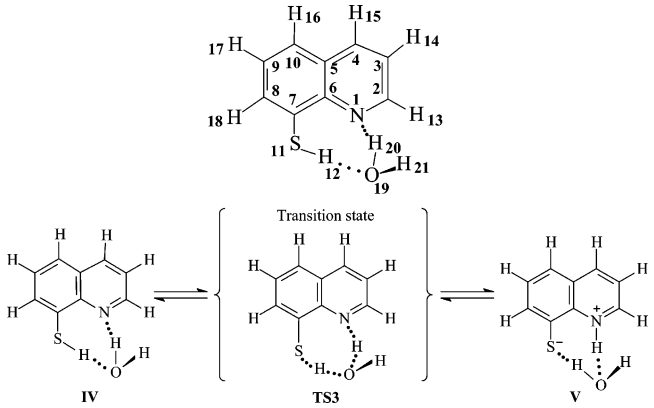

Figure 5. Schematic representation of the complex 8-mercaptoquinoline−H_2O tautomerization.

This problem will be further discussed below on the basis of the energetic parameters of prototropic tautomerism of 8-MQ−H_2O (Figure 8). The complexation energies (E_{HB}), tautomerization energies (ΔE_T), and barrier heights ($\Delta E^{\#}$) in the gaseous phase for different theory levels are listed in Table 10. Imaginary frequencies for TS3 were also computed. The calculated E_{HB} values depend not only upon the electron correlation, but also on the BSSE, which is also presented in Table 10. The potential barriers of the 8-MQ tautomerization (II → III) are 10.185 kcal/mol (MPW1K/6-311++G(d,p)) and 10.257 kcal/mol (B3LYP/6-311++G(d,p)) in the gaseous phase. The corresponding values for one-water complex (IV → V) are close to them and consist of 11.262 kcal/mol (MPW1K/6-311++G(d,p)) and 10.658 kcal/mol (B3LYP/6-311++G(d,p)). The reverse-proton transfer in the complex has a barrier of 4.945 kcal/mol (MPW1K/6-311++G(d,p)) and 5.044 kcal/mol (B3LYP/6-311++G(d,p)) in contrast to the single 8-MQ molecule for which the reverse-proton transfer proceeds essentially without barrier. Consequently, the complexation of 8-MQ with water prevents the transformation of the 8-MQ zwitterionic form into the SH-tautomer. This serves as a prerequisite for predominant existence of 8-MQ in the form of zwitterions that is realized in aqueous solution.[7]

The tautomerization II → III energy is 10.250 kcal/mol (MPW1K/6-311++G(d,p)) and 9.198 kcal/mol (B3LYP/6-311++G(d,p)), and this quantity decreases down to 6.318 and 5.613 kcal/mol at the same theory levels by introducing one water molecule to get 8-MQ−H_2O (IV → V transfer). This is obviously due to the crucial dependence of the tautomerization energy upon the relative stability of the tautomers II and III, which changes under the involvement of the water molecule.

It is impossible to estimate the strength of each of the above-mentioned intermolecular hydrogen bonds, but only a global strength can be obtained that coincides with the reported complexation energy (Table 12).

The geometry parameters of IV, V, and TS3 were optimized for the solutions in different solvents at the MPW1K/6-311++G(d,p) level using the SCRF Onsager method. The geometries in the media with $\epsilon = 2.247$ (benzene) and $\epsilon = 78.39$ (water) are shown in Table 11. For aqueous solution, the N1−H20 distance in IV is 0.021 Å shorter than the corresponding value in the gaseous phase, while the O19−H12 distance is 0.020 Å longer. The partial charges on the S11, N1, and O19 atoms in IV at the MPW1K/6-311++G(d,p) level, according to the Mulliken population analysis, are −0.723, 0.137, and −0.565 in the gaseous phase, and −0.753, 0.142, and −0.591 in the medium with $\epsilon = 78.39$, respectively. Weak hydrogen bonds are mainly electrostatic in nature; the higher negative charge on S11 in the solution makes the attractive electrostatic interactions with the H atom of the extra water molecule stronger than in the gaseous phase, and the distance N1−H20 becomes smaller (Table 11), while the greater positive charge on N1 makes the repulsive interactions in the solution greater than in the gaseous phase and the O19−H12 distance larger. The changes in partial charges on atoms and H-bond lengths

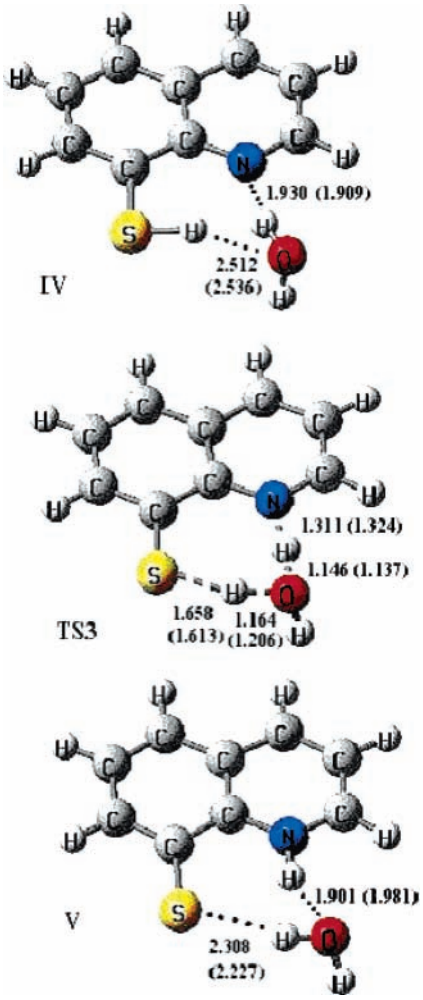

Figure 6. Some interatomic distances (Å) of tautomers IV and V and transition state TS3 at the MPW1K/6-311++G(d,p) level for the gaseous phase and aqueous solution (in parentheses).

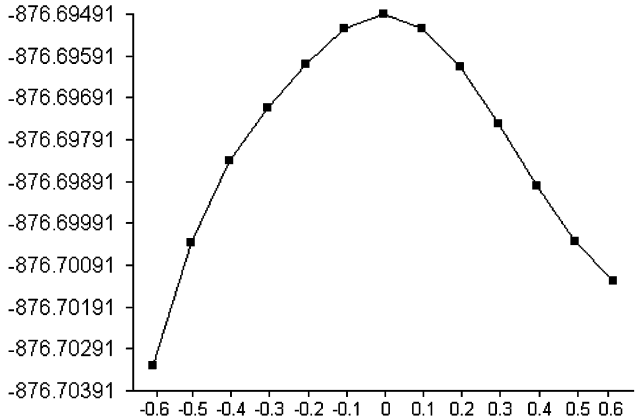

Figure 7. Intrinsic reaction coordinate for 8-mercaptoquinoline water-assisted tautomerization IV → V calculated for the gaseous phase at the B3LYP/6-311++G(d,p) level. The vertical axis is for the total energies in Hartree/particle and the horizontal axis is for reaction coordinate in the units of Bohr.

depending upon the medium correlate well with each other. The results obtained show that the IV form of the 8-MQ−H_2O complex becomes less favorable in aqueous medium compared to that of the gaseous phase (Table 12).

In the aqueous medium, the S11−H12 distance in V is 0.081 Å smaller, while the O19−H20 length is 0.081 Å larger compared to that of the gaseous phase. The partial Mulliken

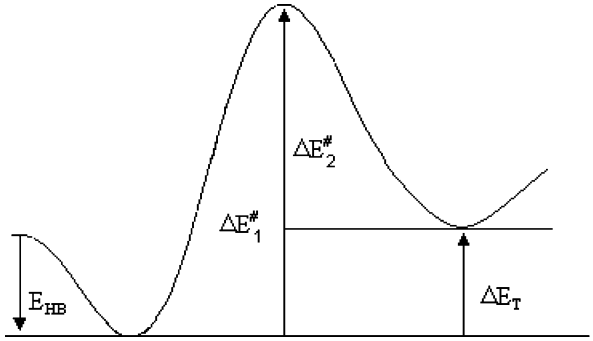

Figure 8. Schematic diagram for the energetics of double-proton transfer in water-assisted tautomerization IV → V of 8-mercaptoquinoline.

charges calculated at the MPW1K/6-311++G(d,p) level are 0.531, −1.424, and −0.462 for N1, S1, and O19 in the gaseous phase, respectively, and 0.477, −1.514, and −0.429, respectively, for the same atoms in the medium with $\epsilon = 78.39$. The higher electron density on S in V makes the hydrogen bond stronger and shorter in passing from the gaseous phase to an aqueous medium. For the structure TS3, the H-bonds with participation of the water oxygen as a hydrogen-bond acceptor become longer with the increasing dielectric constant. The distances O19−H12 and N1−H20 are increased by 0.042 and 0.013 Å, respectively, while the ones S11−H12 and O19−H20 are reduced by 0.046 and 0.008 Å, respectively, in the medium with $\epsilon = 78.39$ compared to that of the gaseous phase. These changes in the H-bond lengths result in the separation of the partial charges of TS3 to increase the dipole moment. The structure TS3 in polar solvent has more polar character than that in the gaseous phase.

The values of the complexation energy (E_{HB}), tautomerization energy (ΔE_T), and barrier heights ($\Delta E^{\#}$) have been calculated at the MPW1K/6-311++G(d,p) level using the SCRF Onsager method (Table 12). The complexation energy in the gaseous phase consists of 5.395 kcal/mol and diminishes with the increase in dielectric constant, being equal to 1.670 kcal/mol in water (at the value $\epsilon = 78.39$). The BSSE corrections depend on the solvent effect. The tautomerization IV → V energy is 6.318 kcal/mol in the gaseous phase and decreases to 2.484 kcal/mol at $\epsilon = 78.39$. The tautomerization energy calculated as a difference of total energies of the solutes (SCRF *E*-field) shows that the V form is more preferable in the aqueous medium. The barrier heights for the double-proton transfer are presented in Table 12. The barrier has a value of 11.262 kcal/mol in the gaseous phase and diminishes in polar medium ($\epsilon = 78.39$) by 2.206 kcal/mol. The reverse proton-transfer barrier is equal to 4.945 kcal/mol in the gaseous phase and increases up to 6.572 kcal/mol in going to the aqueous solution. In general, the results obtained suggest that the water-assisted tautomerization IV → V is facilitated to some extent in polar medium, and the V tautomer is more stable in aqueous solutions compared with IV, which is in agreement with the experimental data.[7]

2.2. NBO Analysis. The nature of the intermolecular hydrogen bonds has been analyzed within the framework of the NBO procedure. The results of the NBO analysis of the second-order perturbation energies corresponding to the hydrogen binding or van der Waals interaction are variously interpreted.[43] The most significant results are concerned with the changes on complexation. The NBO results from Table 13 allow us to make the following comments. In the structure IV, there are two different intermolecular hydrogen binding interactions;, one of

TABLE 10: Complexation Energies (E_{HB}), Tautomerization Energies (ΔE_T), Barrier Heights ($\Delta E^{\#}$), and Imaginary Frequencies for Water-assisted Tautomerization of 8-Mercaptoquinoline in the Gaseous Phase[a]

method	E_{HB}	BSSE	ΔE_T	$\Delta E^{\#}$ IV → V	$\Delta E^{\#}$ V → IV	$\nu^{\#}$ (cm^{-1})
G96LYP/6-311++G(d,p)	−1.659		3.969	7.332	3.363	−1202.89
B3LYP/6-311++G(d,p)	−4.638 (−4.248)[b]	0.391	5.613	10.658	5.044	−1327.22
MPW1K/6-311++G(d,p)	−5.395 (−4.945)	0.452	6.318	11.262	4.945	−1264.33
BH&HLYP/6-311++G(d,p)	−5.100 (−4.739)	0.363	7.993	15.699	7.706	−1401.30

[a] Energies in kcal/mol including ZPE corrections. [b] The BSSEs are involved.

TABLE 11: Geometry Parameters for Monohydrated 8-Mercaptoquinoline at the MPW1K/6-311++G(d,p) Level in Solvents[a]

	$\epsilon = 2.247$[b]	Δ[c]	$\epsilon = 78.39$	Δ[c]
Geometry Parameters for IV				
N1−C6	1.351	0.001	1.352	0.002
C6−C7	1.422	0.000	1.421	−0.001
S11−C7	1.756	0.001	1.759	0.004
N1−H20	1.919	−0.011	1.909	−0.021
S11−H12	1.337	0.000	1.337	0.00
O19−H12	2.505	−0.006	2.537	0.020
O19−H20	0.965	0.002	0.967	0.004
∠(S11−H12−O19)	144.964	0.177	142.778	−2.009
∠(N1−H20−O19)	170.797	2.657	172.619	4.479
∠(H20−O19−H12)	49.278	0.202	48.684	−0.612
Geometry Parameters for TS3				
N1−C6	1.359	0.001	1.359	0.001
C6−C7	1.431	0.000	1.430	−0.001
S11−C7	1.747	0.005	1.754	0.012
N1−H20	1.318	0.007	1.324	0.013
S11−H12	1.642	−0.017	1.613	−0.046
O19−H12	1.179	0.015	1.206	0.042
O19−H20	1.141	−0.005	1.138	−0.008
∠(S11−H12−O19)	165.942	0.467	166.511	−1.036
∠(N1−H20−O19)	172.858	−0.029	172.687	−0.200
∠(H20−O19−H12)	86.301	−0.079	85.991	−0.389
Geometry Parameters for V				
N1−C6	1.352	0.002	1.355	−0.005
C6−C7	1.427	0.000	1.425	−0.002
S11−C7	1.717	0.006	1.730	−0.019
N1−H20	1.024	−0.001	1.021	−0.004
S11−H12	2.286	−0.022	2.227	−0.081
O19−H12	0.971	0.001	0.973	0.003
O19−H20	1.911	0.011	1.981	0.081
∠(S11−H12−O19)	152.205	2.718	157.337	7.310
∠(N1−H20−O19)	157.694	1.880	154.980	−0.160
∠(H20−O19−H12)	71.599	−0.240	69.222	−2.617

[a] Atoms are assigned the same numbers as in Figure 5. Lengths are in Å, angles are in degrees. [b] Dielectric constant. [c] Deviations from gaseous-phase geometries.

these is considerably stronger than another. The Fock matrix analysis for IV using the second-order perturbation theory shows that the interaction of the lone pair of O19 and the S11−H12 antibonding orbital leads to stabilization energy of 1.27 kcal/mol, while the interaction of the lone pair of N1 and the O19−H20 antibonding orbital stabilized the system by 10.30 kcal/mol. In this complex IV, $\sigma^*_{O19-H20}$ and $\sigma^*_{S11-H12}$ antibonds participate as acceptors, with the lone pairs of oxygen and nitrogen as donors in the intermolecular charge transfer. The n_N and n_O occupation numbers diminish with respect to the isolated molecules. As a result, the $\sigma^*_{O19-H20}$ antibond occupation number increases by 0.02275 e, and this change is accompanied by a contraction of the O19−H20 bond. The change in $\sigma^*_{S11-H12}$ is just the reverse, i.e., its occupation number decreases by 0.01448 e, and the elongation of the S11−H12 distance occurs on complexation. The corresponding NBO second-order perturbation energies for IV in aqueous solution (SCRF Onsager model) are 1.11 and 11.87 kcal/mol (the case IVa in Table 13). The structure V has two characteristic intermolecular bonds S···O−H and O···N−H. As seen from Table 13, the stabilization energy caused by the interaction between the lone pair of S11 and the antibonding orbital of O12−H19 is 11.67 kcal/mol, whereas the lone pair of O19 interacts with the antibond N1−H20 to yield 12.06 kcal/mol. The contributions from the latter two quantities to V[a] consists of 16.00 and 10.71 kcal/mol, respectively. Therefore, the tautomer V is more stable in aqueous solution compared to that of the gaseous phase. In the structure V in the gaseous phase, on complexation with a water molecule, the $\sigma^*_{O19-H12}$ antibond occupancy increases from 0.00001 to 0.03974 e, and this bond contracts. The occupation number of the sulfur lone pair orbital decreases by the comparable value. It is notable that, despite the strong intermolecular interaction $n_O \rightarrow \sigma^*_{N1-H20}$ and the reduction of n_O occupation number on complexation compared to that of the isolated molecule III, the value of the σ^*_{N1-H20} occupation number diminishes with respect to the isolated molecule in both the gaseous phase and aqueous solution. The energy of $n_O \rightarrow \sigma^*_{N1-H20}$ interaction is 1.35 kcal/mol lower in aqueous medium than in the gaseous phase; therefore, the σ^*_{N1-H20} antibond occupation number increases appreciably, but the bond N1−H20 length remains unchanged.

It is probable that an isolated zwitterionic thiolate (like V) should have an extremely strong intramolecular H-bond resonance of the S···H−N type. This would correspond to a great NRT contribution of resonance forms of the S−H···N$^-$ or S···H$^+$···N type to a severe $n_S \rightarrow \sigma^*_{N1-H20}$ delocalization. The zwitterionic character (particularly, diffuse, of p-type, radial to a considerable extent, lone pair of the sulfur atom) enhances such intramolecular delocalization in the σ-system. When the H_2O molecule becomes involved in the interaction, the two intermolecular H-bonds (S···H−O and O···H−N) are evidently sufficient to disrupt one intramolecular S···H−N bond. But on the reverse exchange, in the interaction with σ^*_{N1-H20} orbital, the neutral O atom from water is a weaker Lewis base than the anionic S$^-$ center, so the occupancy of σ^*_{N1-H20} is somewhat reduced in the complex, as it is observed.

The results of NBO analysis indicate that the interactions in the structure V are stronger than those in structure IV. The last assumption is confirmed by the larger stability of tautomer V compared with that of IV (Table 12 and ref 7).

Conclusion

First of all, we have studied the IHB formation, conformational equilibrium, rotational barriers, single-proton transfer in the tautomerization reaction, and charge distribution in 8-MQ in the gaseous phase and in solution using different DFT methods. The most strict calculation of the IHB energy was achieved using the MPW1K/6-311++G(d,p) theory level. Our computations have shown also that the allowance for diffuse functions is quite necessary for full characterization of the hydrogen-bond interaction. Two SCRF models were used for the account of solvent effects. It has been demonstrated that

TABLE 12: Complexation Energies (E_{HB}), Tautomerization Energies (ΔE_T), Barrier Heights ($\Delta E^{\#}$), and Imaginary Frequencies for Water-assisted Tautomerization in the Gaseous Phase and in Solutions at the MPW1K/6-311++(d,p) Level within the Onsager SCRF Method[a]

						$\Delta E^{\#}$		
solvent	ϵ[b]	E_{HB}	BSSE	ΔE_T	ΔE_{T-SCRF}[d]	IV → V	V → IV	$\nu^{\#}$ (cm^{-1})
gaseous phase	1	−5.395 (−4.945)[c]	0.450	6.318		11.262	4.945	−1264.33
benzene	2.247	−2.461 (−1.717)	0.744	5.122	3.614	10.445	5.324	−1293.35
dichloroethane	10.36	−1.914 (−0.918)	0.996	3.348	−4.257	9.518	6.170	−1330.76
ethanol	24.55	−1.763 (−0.588)	1.175	2.812	−6.101	9.228	6.416	−1339.63
nitromethane	38.2	−1.680 (−0.412)	1.268	2.604	−6.807	9.101	6.497	−1341.35
water	78.39	−1.670 (−0.382)	1.288	2.484	−7.735	9.056	6.572	−1343.51

[a] Energies in kcal/mol including ZPE corrections. Complexation energies are given for the structure IV. [b] Dielectric constant. [c] Numbers in parentheses represent the BSSE-corrected E_{HB} values. [d] Tautomerization energies as differences of total energies of solute (SCRF *E*-field).

TABLE 13: NBO Analysis (MPW1K/6-311++G(d,p)) of Complexes IV−V: Occupation Numbers of the σ^*_{X-H} Antibonds, n_N, n_O and n_S Lone Pairs (the same parameters for the isolated compounds are given in parentheses; the values in square brackets are Wiberg bond orders for complex and isolated molecules, respectively); the Nature of Donor Orbitals ϕ_i, Acceptor Orbitals ϕ_j, and the Second-order Perturbation Energies $\Delta E_{ij}^{(2)}$ in kcal/mol

	n_N	n_O	n_S	$\sigma^*_{O19-H20}$	$\sigma^*_{S11-H12}$	$\sigma^*_{O19-H12}$	σ^*_{N1-H20}	$\phi_i \rightarrow \phi_j$	$\Delta E_{ij}^{(2)}$
IV	1.90510	1.99076		0.02275 [0.735]	0.01448 [0.948]			LP(N1) → BD*(O19− H20)	10.30
	(1.90892)	(1.99678)		(0.00001) [0.793]	(0.020) [0.937]			LP(O19) → BD*(S11− H12)	1.27
IV[a]	1.90306	1.99143		0.02633 [0.723]	0.01432 [0.951]			LP(N1) → BD*(O19− H20)	11.87
	(1.90764)	(1.99700)		(0.00000) [0.782]	(0.02217) [0.933]			LP(O19) → BD*(S11− H12)	1.11
V		1.97081	1.98327			0.03974 [0.697]	0.06496 [0.662]	LP(S11) → BD*(O19− H12)	11.67
		(1.99678)	(1.98562)			(0.00001) [0.793]	(0.10018) [0.6368]	LP(O19) → BD*(N1− H20)	12.06
V[a]		1.97309	1.98329			0.05000 [0.688]	0.05373 [0.685]	LP(S11) → BD*(O19− H12)	16.00
		(1.99700)	(1.98729)			(0.00000) [0.782]	(0.06689) [0.684]	LP(O19) → BD*(N1− H20)	10.71

[a] The complex was calculated in aqueous solution using the SCRF Onsager model.

the form III is more stable in polar solutions compared to that of II. The forward proton transfer from II to III occurs with a barrier of about 10.5 kcal/mol and the reverse-proton transfer almost without any barrier at all. The probability of II → III tautomerization in the gaseous phase is low. However, the barrier height and tautomerization (II → III) energy decrease in aqueous solution by 2.741 and 7.033 kcal/mol, respectively.

The aforementioned reaction is thermodynamically more preferable in polar medium compared to that of the gaseous phase. As for the kinetic aspect, a polar solvent makes the barrier of II → III transfer somewhat lower, the barrier of the reverse process substantially higher. Consequently, their natural explanation get the displacement of 8-MQ tautomeric equilibrium in aqueous medium toward a zwitterionic form, as well as the improvement of kinetic conditions for the zwitterization process in aqueous solution compared with that of the solutions in nonpolar solvents.[7]

Therefore, among all the energetic criteria (Table 4), only those intrinsic for the SCRF approach (total energy of the polarized solute for the PCM and total energy of solute within the Onsager model) reproduce the known values from the experiments'[7] thermodynamic preference of the tautomer III in aqueous solution compared with that of II.

The double-proton transfer in water-assisted tautomerization of 8-MQ−H_2O occurs concertedly and synchronously both in the gaseous phase and in solution. All the results indicate that the tautomers IV and V exist in the form of the hydrogen-binding clusters. The TS3 structure in polar solvent has more polar character than in the gaseous phase. The symmetry of the transition state does not change with solvent. An extra single water molecule in the structure reduces the barrier height for the process IV → V by 2.206 kcal/mol and the tautomerization energy for the double-proton transfer by 3.834 kcal/mol in solution compared to that of the gaseous phase. We have shown that the IV → V reaction is preferable kinetically and thermodynamically in a polar solution. In general, the water-assisted tautomerization is kinetically less favorable but thermodynamically more favorable in comparison with the single-proton transfer. The values of ΔE_T and $\Delta E^{\#}_{IV\rightarrow V}$ decrease with a dielectric constant growth, and therefore, the water-assisted tautomerization becomes more favorable in polar solvent.

Like for the separate 8-MQ tautomerization, the thermodynamics of the water-assisted process is described more adequately by means of the Onsager total energy of solute than using a sum of electronic and zero-point energies.

The BSSEs of E_{HB} depend to some extent on the dielectric constant and theory level. NBO analysis has been performed to explore the nature of the bonds in the complexes. It has been revealed that the strongest intermolecular interaction involving charge transfer from S11 to the antibond $\sigma^*_{O19-H12}$ takes place in aqueous solution. As a consequence, the occupation number of the just-mentioned antibond is relatively high, and concomitantly, a contraction of O19−H12 bond is observed.

As we have found earlier (unpublished data), in the case of 8-hydroxyquinoline, the series of stability of all the forms in gaseous phase remains the same in solution. We can suggest in this respect that, despite the important role of the solvent electrostatic effects, the intrinsic stability of those species overcomes the solvent effects. On the contrary, the results of

the present work show that for 8-MQ the effects of polar solvent exert the decisive influence on the relative stability of different tautomers.

Acknowledgment. We would like to thank Professor Frank A. Weinhold (Department of Chemistry, University of Wisconsin, Madison, U.S.A.), Professor Ruslan M. Minyaev (Laboratory of Quantum Chemistry, Scientific Research Institute of Physical and Organic Chemistry, Rostov State University, Rostov-on-Don, Russia), and Ph. D. Olga M. Tsivileva (Laboratory of Microbiology and Mycology, Institute of Biochemistry and Physiology of Plants and Microorganisms, Russian Academy of Sciences, Saratov, Russia) for valuable advice and discussion.

References and Notes

(1) Albert, A.; Barlin, G. B. *J. Chem. Soc*. **1959**, 2384−2396.
(2) Kealey, D.; Freiser, H. *Anal. Chem.* **1966**, *38*, 1577−1581.
(3) Spinner, E. *J. Chem Soc.* **1960**, 1237−1242.
(4) Ashaks, Ya. V.; Sturis, A. P.; Bankovskii, Yu. A.; Ievin'sh, A. F. *Izv. Akad. Nauk LatvSSR., Ser. Khim.* **1967**, 427−432.
(5) Bankovskii, Yu. A.; Chera, L. M.; Ievin'sh, A. F. *Zh. Anal. Khim.* **1964**, *19*, 414−424.
(6) Bankovskii, Yu. A. *Izv. Akad. Nauk LatvSSR., Ser. Khim.* **1970**, 643−652.
(7) Bankovskii, Yu. A. *Chemistry of Internal Complex Compounds of 8-Mercaptoquinoline and Its Derivatives (in Russian)*; Zinatne: Riga, 1978.
(8) Li, Quan-Song; Fang, Wei-Hai. *Chem. Phys. Lett.* **2003**, *367*, 637−644.
(9) Frisch, M. J.; Trucks, G. W.; Schlegel, H. B.; Scuseria, G. E.; Robb, M. A.; Cheeseman, J. R.; Zakrzewski, V. G.; Montgomery, J. A., Jr.; Stratmann, R. E.; Burant, J. C.; Dapprich, S.; Millam, J. M.; Daniels, A. D.; Kudin, K. N.; Strain, M. C.; Farkas, O.; Tomasi, J.; Barone, V.; Cossi, M.; Cammi, R.; Mennucci, B.; Pomelli, C.; Adamo, C.; Clifford, S.; Ochterski, J.; Petersson, G. A.; Ayala, P. Y.; Cui, Q.; Morokuma, K.; Malick, D. K.; Rabuck, A. D.; Raghavachari, K.; Foresman, J. B.; Cioslowski, J.; Ortiz, J. V.; Stefanov, B. B.; Liu, G.; Liashenko, A.; Piskorz, P.; Komaromi, I.; Gomperts, R.; Martin, R. L.; Fox, D. J.; Keith, T.; Al-Laham, M. A.; Peng, C. Y.; Nanayakkara, A.; Gonzalez, C.; Challacombe, M.; Gill, P. M. W.; Johnson, B. G.; Chen, W.; Wong, M. W.; Andres, J. L.; Head-Gordon, M.; Replogle, E. S.; Pople, J. A. *Gaussian 98*, revision A.7; Gaussian, Inc.: Pittsburgh, PA, 1998.
(10) Becke, A. D. *J. Chem. Phys.* **1993**, *98*, 5648−5652.
(11) Lee, C.; Yang, W.; Parr, R. G. *Phys. Rev.* **1988**, *B37*, 785−789.
(12) Lynch, B. J.; Fast, P. L.; Harris, M.; Truhlar, D. G. *J. Phys. Chem.* **2000**, *A104*, 4811−4815.
(13) Frisch, A.; Frisch, M. J. *Gaussian 98 Users Reference*; Gaussian Inc.: Pittsburgh, PA, 1998; p 75.
(14) Adamo, C.; Barone, V. *J. Comput. Chem*. **1998**, *19*, 418−429.
(15) Schlegel, H. B.; McDouall, J. J. In *Computational Advances in Organic Chemistry*; C. Ogretir, C., Csizmadia, I. G., Eds.; Kluwer Academic: The Netherlands, 1991.
(16) Ditchfield, R.; Hehre, W. J.; Pople, J. A. *J. Chem. Phys*. **1971,** *54*, 724−728.
(17) Clark, T.; Chandrasekhar, J.; Spitznagel, G. W.; Schleyer, P. v. R. *J. Comput. Chem*. **1983**, *4*, 294−301.
(18) Frisch, M. J.; Pople, J. A.; Binkley, J. S. *J. Chem. Phys*. **1984**, *80*, 3265−3269.
(19) McLean, A. D.; Chandler, G. S. *J. Chem. Phys.* **1980**, *72*, 5639−5648.
(20) Krishnan, R.; Binkley, J. S.; Seeger, R.; Pople, J. A. *J. Chem. Phys.* **1980**, *72*, 650−654.
(21) Peng, C.; Schlegel, H. B. *Isr. J. Chem.* **1994**, *33*, 449−454.
(22) Schlegel, H. B. *Theor. Chim. Acta* **1984**, *66*, 333−340.
(23) Gonzalez, C.; Schlegel, H. B. *J. Phys. Chem.* **1990**, *94*, 5523−5527.
(24) Glendening, E. D.; Reed, A. E.; Carpenter, J. E.; Weinhold, F. A. *NBO, version 3.1*, 1995.
(25) Boys, S. F.; Bernardi, F. *Mol. Phys*. **1970**, *19*, 553−566.
(26) Tapia, O. In *Molecular Interaction*; Ratajczak, H., Orville-Thomas, W. J., Eds.; Wiley: New York, 1982; Vol. 3, p 47.
(27) Onsager, L. *J. Am. Chem. Soc.* **1936**, *58*, 1486-1493.
(28) Amovilli, C.; Barone, V.; Cammi, R.; Cances, E.; Cossi, M.; Mennucci, B.; Pomelli, C. S.; Tomasi, J. *Adv. Quantum Chem.* **1998**, *32*, 227−262.
(29) Barone, V.; Cossi, M.; Mennucci, B.; Tomasi, J. *J. Chem. Phys.* **1997**, *107*, 3210−3221.
(30) Bankovskii, Yu. A.; Zuika, I. V.; Tsirule, Ya. A.; Tsirule, M. A. *Izv. Akad. Nauk LatvSSR., Ser. Khim.* **1971**, 276−290.
(31) Katritzky, A. R., Jones, R. A. *J. Chem. Soc.* **1960**, *7*, 2942−2947.
(32) Zuika, I. V.; Bankovskii, Yu. A.; Krasovska, M. E.; Ievin'sh, A. F. *Izv. Akad. Nauk LatvSSR., Ser. Khim.* **1968**, 242−243.
(33) Panchenko, Yu. N. *Zh. Strukt. Khim***. 1999**, *40*, 548−555.
(34) Yoshida, H.; Ehara, A.; Matsuura H. *Chem. Phys. Lett.* **2000**, 325, 477−483.
(35) Davidson, E. R. *Int. J. Quantum Chem*. **1998**, *69*, 241−245.
(36) Zuika, I. V.; Bankovskii, Yu. A.; Sturis, A. P.; Zaruma, D. E.; Tsirule, Ya. A.; Tsirule, M. A. *Izv. Akad. Nauk LatvSSR., Ser. Khim.* **1971**, 650−658.
(37) Zuika, I. V.; Bankovskii, Yu. A. *Izv. Akad. Nauk LatvSSR., Ser. Khim.* **1972**, 668−672.
(38) Lynch, B. J. Truhlar, D. G. *J. Phys. Chem.* **2001**, *A105*, 2936−2941.
(39) Mulliken, R. S. *J. Chem. Phys.* **1955**, *23*, 1833−1840.
(40) Bankovskii, Yu. A.; Zuika, I. V. *Izv. Akad. Nauk LatvSSR., Ser. Khim.* **1969**, 412−421.
(41) Zuika, I. V.; Bankovskii, Yu. A.; Pruvers, Z. P.; Sturis, A. P.; Zaruma, D. E.; Krasovska, M. E. *Izv. Akad. Nauk LatvSSR., Ser. Khim.* **1977**, 746−747.
(42) Hobza, P.; Havlas, Z. *Chem. Rev.* **2000**, *100*, 4253−4264.
(43) Reed, A. E.; Curtiss, L. A.; Weinhold, F. A. *Chem. Rev*. **1988**, *88*, 899−926.